Proceedings IRF2020: 7th International Conference Integrity-Reliability-Failure.
J.F. Silva Gomes and S.A. Meguid (editors), INEGI-FEUP (2020), pp.917-930.
https://paginas.fe.up.pt/~irf/Proceedings_IRF2020/

PAPER REF: 17777

INFLUENCE OF A TMD IN ITS CONTROL ACTION OF A SDOF FRAME WITH NON-LINEAR HYSTERETIC BEHAVIOR

Pedro Folhento[1], Manuel Braz-César[2], António Paula[2], Rui C. Barros[1(*)]

[1]Faculty of Engineering of the University of Porto, Rua Roberto Frias, Porto, Portugal
[2]Polytechnic Institute of Bragança, Campus de Santa Apolónia, Bragança, Portugal
[(*)]*Email:* rcb@fe.up.pt

ABSTRACT

This paper presents a parametric investigation concerning the control parameters of a Tuned Mass Damper (TMD), with the purpose of reducing vibrations of a SDOF frame structure with non-linear hysteretic behaviour, when it is subjected to earthquakes and wind loads. A numerical model (MATLAB/Simulink) is implemented in order to obtain the structural response of a SDOF infilled wall frame structure subjected to two different acceleration signals and evaluate the effectiveness of the applied TMD when the value of its mass is changed. Four different hysteretic behaviour cases will be considered for the infilled wall frame structure. Based on the results obtained, the definition of the mass ratio between the TMD and the main structure will be crucial in finding the ideal performance of a TMD.

Keywords: non-linear behaviour, hysteresis, passive control systems, tuned mass dampers.

INTRODUCTION

Civil structures exhibit non-linear and complex behaviour that are usually linearized to simplify the design procedure. For instance, disregarding non-structural elements constitutes one of the design procedure simplifications that are commonly implemented. When dynamic loads, such as seismic and wind excitations act on framed structures it requires the structural control of the lateral displacements in the structure. In these situations, the presence of non-structural elements highly influences the behaviour and so, the response of the corresponding framed structure. This simplification must be then assed in whether is appropriate to design passive control systems for building structures.

Tuned mass dampers (TMDs) are well-known passive control systems whose main purpose is to reduce building vibrations due to lateral loads. They increase the energy dissipation capacity of the structure in which they are applied. A typical model representation is represented in Figure 1 and consists on a primary mass, considered to be the main structure, in which a secondary and smaller mass is applied, considered to be the TMD.

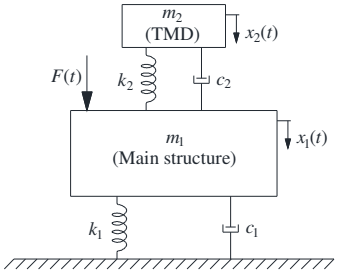

Fig. 1 - Typical model representation for the system Structure+TMD.

Tuning the control parameters of a TMD requires knowledge about the dynamic structure properties. Non-linear behaviour can compromise the overall performance of the control system. Therefore, to better define certain control parameters in the design procedure an investigation is carried out regarding the implementation of TMDs in a single degree-of-freedom (SDOF) frame structure with four different cases of non-linear behaviour for the non-structural element.

NUMERICAL MODELLING

Figure 3(a) presents the schematic representation used for the present investigation consisting on the SDOF frame structure that when applying the TMD it becomes a two degree-of-freedom (2DOF) system, being m_1 the mass of the single-story framed structure and m_2 the TMD mass. The frame structure is connected to the exterior by a spring of stiffness k_1, and by a damping constant c_1. In like manner, the TMD is connected to the main structure by a spring of stiffness k_2, and by a damping constant c_2.

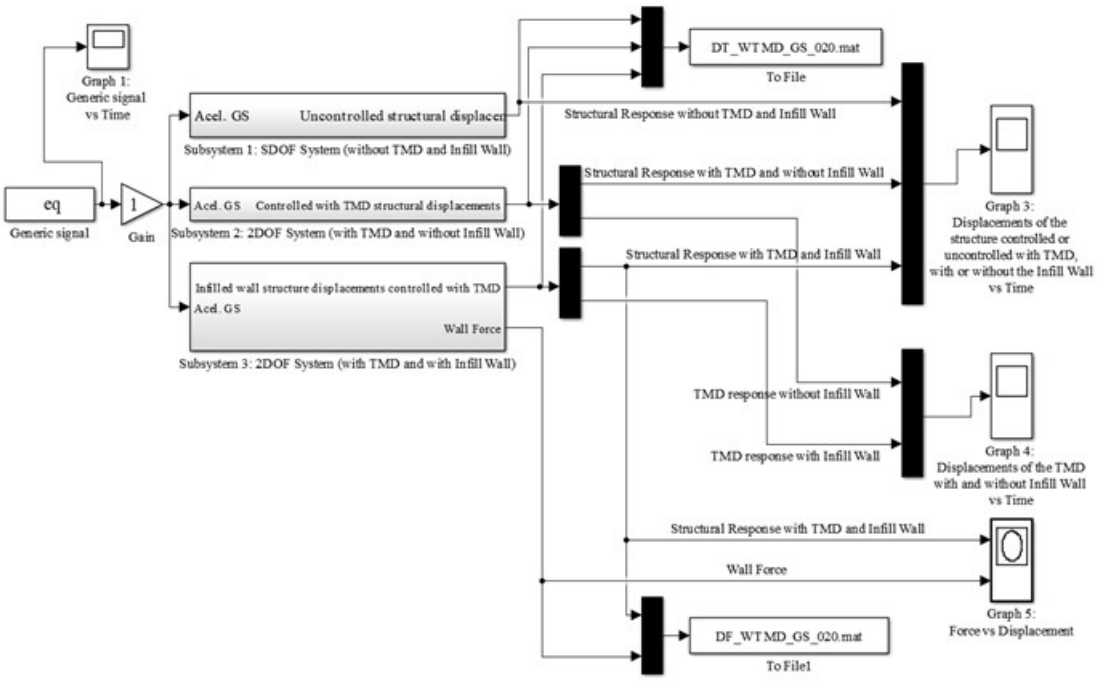

Fig. 2 - Macro-Simulink model used for the present investigation.

A Simulink model was implemented based on the properties of the structural system. It was considered in this study the following parameters: mass of the structure m_1=5000kg; the period T=1.0s and the structural damping coefficient ξ =0.05 [1].

The Macro-Simulink numerical model used in this investigation (Figure 2) was adapted from Mousavi *et al.* [2], and is based on a smooth hysteretic model that was first suggested by Bouc [3] (and developed by many others: Wen [4], Baber and Noori [5], Casciati [6], Reinhorn *et al.* [7], Sivaselvan and Reinhorn [8].

To assess the performance of the TMD applied on the infilled wall structure, sketched in Figure 3(a), four cases of hysteretic behaviour of the representative non-structural wall were considered: a plain hysteretic behaviour without any degradation; stiffness degradation only; stiffness and strength degradation; and stiffness and strength degradation with the pinching effect.

For the different cases of hysteretic behaviour, the parameter that controls the mass ratio between the TMD and the main structure was changed in order to find an optimal controlled response, considering the following values: μ=0.05; μ=0.10; μ=0.15; and μ=0.20.

Two acceleration signals will be used in this investigation. The first one, shown in Figure 3(b), is a harmonic generic signal with different acceleration values. The second acceleration signal, shown in Figure 3(c), is the ground acceleration of the well-known El Centro earthquake.

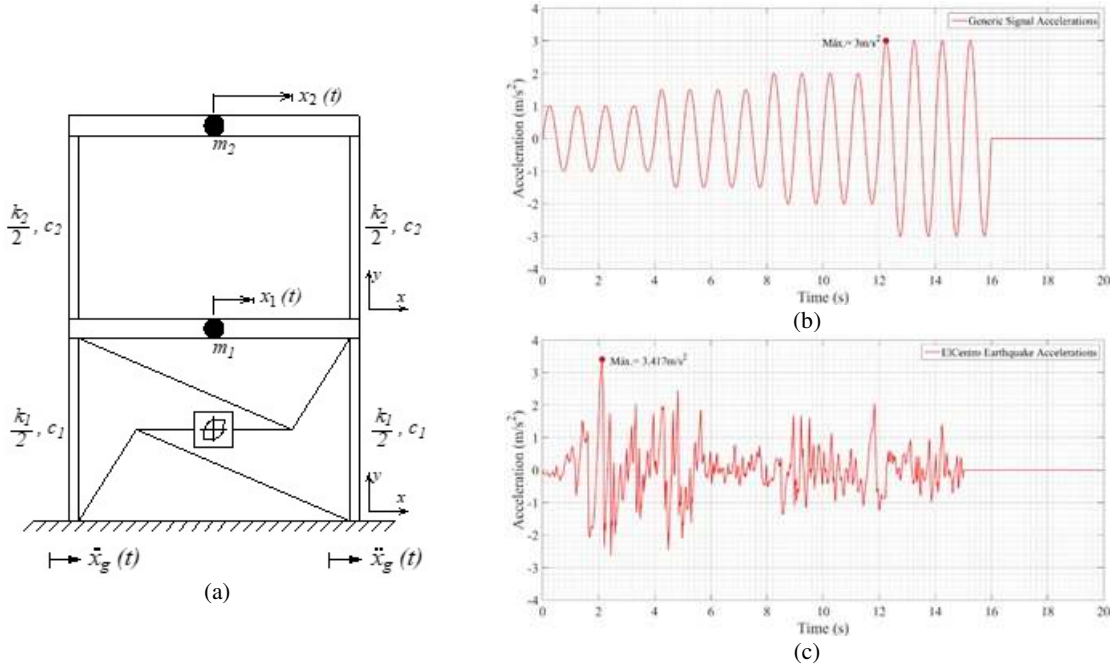

Fig. 3 - (a) Schematic representation of the 2DOF system; (b) Generic harmonic acceleration signal; (c) Seismic acceleration signal - El Centro's Earthquake. Source: Folhento [1]

Table 1 - Hysteretic parameters to simulate the different frame behaviours (N=3; a=0.03; η=5)

Case	Hysteretic behaviour	α	β_1	β_2	σ	R_{sp}	λ_c	κ
0	Plain hysteretic behaviour	50	0	0	1	0	0	0
1	Stiffness degradation	1	0	0	1	0	0	0
2	Stiffness and strength degradation	1	0.3	0.3	1	0	0	0
3	Stiffness and strength degradation with pinching effect	1	0.3	0.3	0.2	0.1	0	0.5

Source: Mousavi *et al.* [2]

Table 1 presents the hysteretic parameters and their respective values for the different cases of hysteretic behaviour of the representative infill wall considered in the present study.

FRAME HYSTERETIC BEHAVIOUR

To represent the hysteretic behaviour of the frame with infill wall, the numerical model aforementioned (Figure 2) is used to draw the several hysteretic loops characterized by the different cases of hysteretic behaviour considered. It will always be represented the TMD controlled hysteretic loops in bold and in blue colour for the various mass ratios considered along with the corresponding uncontrolled hysteretic loops in a faded grey colour.

CASE 0: PLAIN HYSTERETIC BEHAVIOUR

In this case of hysteretic behaviour, no degradation is considered, is suitable for well-detailed steel structures, and it is represented by the following equations

$$P_f = k_f\, x = (a k_0 + k_{hyst})\, x$$
$$k_{hyst} = (1-a)\, k_0 \left\{ 1 - \left| \frac{P_f}{P_{fy}} \right|^N \left[\eta\, \mathrm{sgn}\left((1-a) P_f\, \dot{x} \right) + 1 - \eta \right] \right\} \quad (1)$$

where k_f is the nonlinear total lateral stiffness of the frame, k_0 is its initial lateral stiffness, "a" is the post-yield stiffness ratio, "N" a parameter that controls the transition smoothness from pre-yield to post-yield and η controls the shape of the unloading path. P_f and P_{fy} are the current frame shear and its yield value, respectively. Additionally, sgn is the signum function.

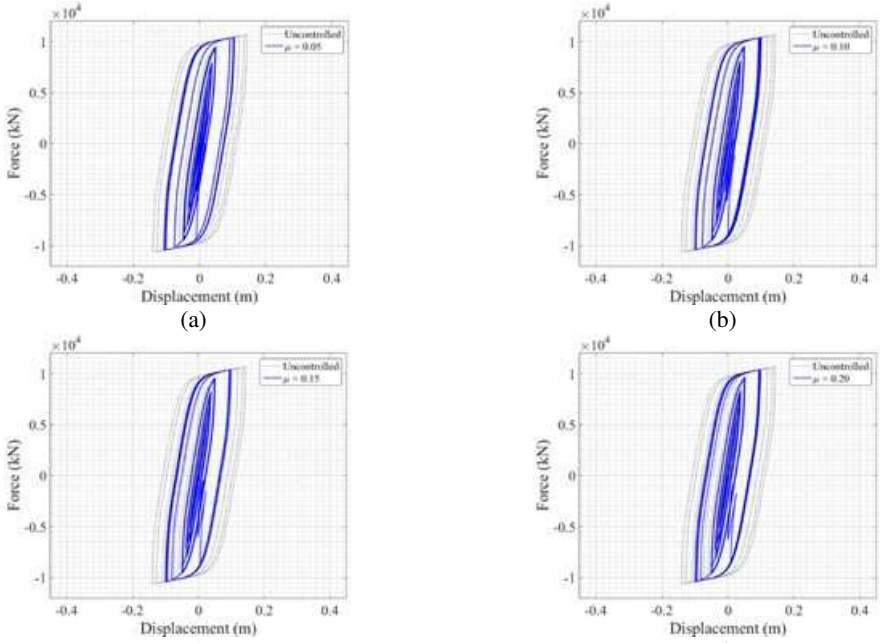

Fig. 4 - Hysteretic loops of the infilled wall frame structure under the generic harmonic signal acceleration, considering a plain hysteretic behaviour (Case 0): a) Mass Ratio of 5%; b) Mass Ratio of 10%; c) Mass Ratio of 15%; d) Mass Ratio of 20%

The graphs of Figure 4 present the hysteretic loops controlled and uncontrolled with the TMD for the plain hysteretic behaviour. Four graphs are shown, each representing one different value of the mass ratio between the TMD and the main structure.

CASE 1: STIFFNESS DEGRADATION

Stiffness degradation is due to geometric effects. Elastic stiffness decreases with increased ductility. The stiffness degradation is created in the Macro-Simulink model through the so-called pivot rule [9]. Most reinforced concrete undergoes stiffness degradation that should be considered in a nonlinear dynamic analysis. To address this case, k_{hyst} should be modified as follows

$$k_{hyst} = (R_k - a)\, k_0 \left\{ 1 - \left| \frac{P_f}{P_{fy}} \right|^N \left[\eta\, \mathrm{sgn}\left((1-a) P_f\, \dot{x} \right) + 1 - \eta \right] \right\} \quad (2)$$

where

$$P_f = k_f\, x = (a k_0 + k_{hyst})\, x$$
$$R_k = \frac{P_f + \alpha P_{fy}}{k_0\, x + \alpha P_{fy}} \quad (3)$$

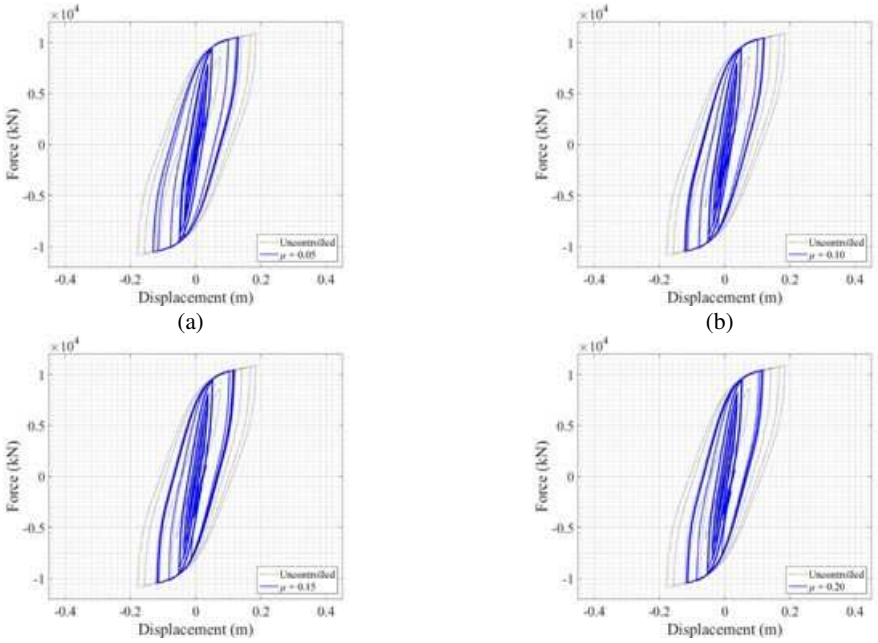

Fig. 5 - Hysteretic loops of the infilled wall frame structure under the generic harmonic signal acceleration, considering the stiffness degradation (Case 1): a) Mass Ratio of 5%; b) Mass Ratio of 10%; c) Mass Ratio of 15%; d) Mass Ratio of 20%

Parameter α can control the stiffness degradation, i.e., the higher the α, the lower the stiffness degradation. Parameter R_k is always a positive value and the unit is its maximum possible value. However, R_k is also a decreasing function of time, since the stiffness of the structure would not increase after deterioration, regardless of the current displacement.

Figure 5 shows the graphs representing the hysteretic loops of the infilled wall frame structure with stiffness degradation. Each graph presents the uncontrolled hysteretic loop and the corresponding controlled case with a different value of the TMD mass.

CASE 2: STIFFNESS AND STRENGTH DEGRADATION

To counteract the P-Δ effects, as well as the strength deterioration during repeated load reversals, degradation of resistance based on energy/ductility is implemented in the Macro-Simulink model. This is achieved by the following modification on the yield strength.

$$P_{fy} = P_{fy0}\left[1-\left(\frac{x_{max}}{x_{ult}}\right)^{\frac{1}{\beta_1}}\right]\left[1-\frac{\beta_2 H}{(1-\beta_2)H_{ult}}\right] \tag{4}$$

The degraded and initial yielding strength of the frame are indicated by P_{fy} and P_{fy0}, respectively. The parameters u_{max} and u_{ult} are the maximum displacement in the current load inversion and the ultimate displacement capacity of the frame, respectively. The dissipated energy accumulated at the current displacement is represented by H and H_{ult} is the ultimate dissipated energy under monotonic (non-cyclic) load. Furthermore, β_1 and β_2 are degradation parameters based on ductility and energy dissipation demands, respectively.

Strength degradation should be considered for intermediate moment resisting frames under great ductility demands. Most reinforced concrete frames and shear walls would also experience strength deterioration.

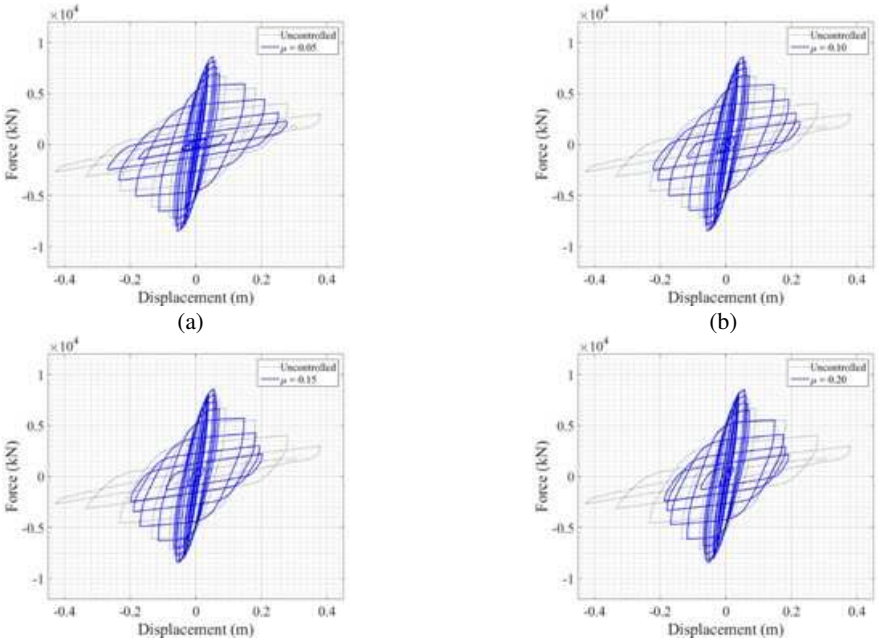

Fig. 6 - Hysteretic loops of the infilled wall frame structure under the generic harmonic signal acceleration, considering the stiffness and strength degradation (Case 2): a) Mass Ratio of 5%; b) Mass Ratio of 10%; c) Mass Ratio of 15%; d) Mass Ratio of 20%

The graphs of Figure 6 present the controlled and uncontrolled hysteretic loops for the hysteretic case of stiffness and strength degradation, for the different values of the mass ratio considered in the present study.

CASE 3: STIFFNESS AND STRENGTH DEGRADATION WITH PINCHING

Most of reinforced concrete shear walls and structures with masonry infill walls revealed compressed (or pinched) hysteretic cycles in early tests [2].

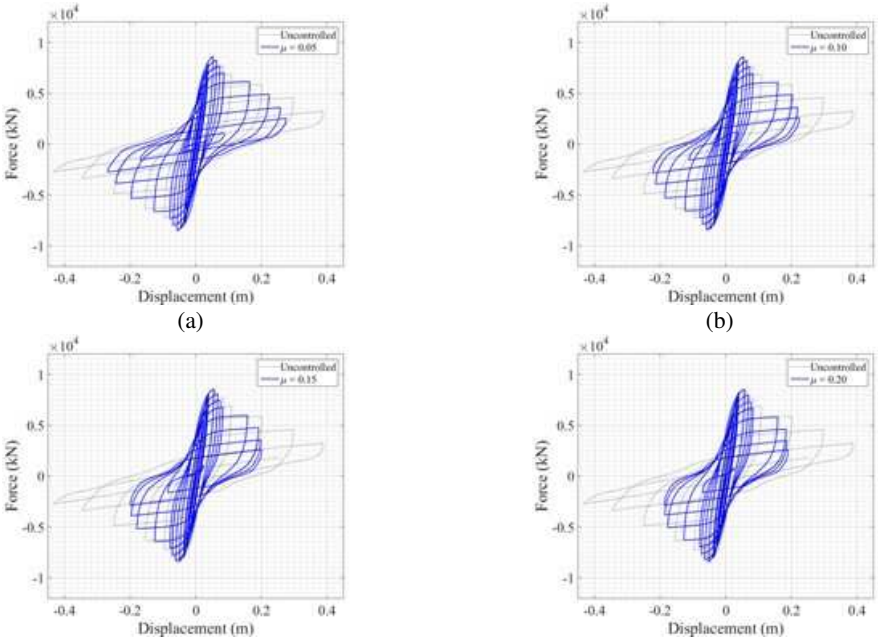

Fig. 7 - Hysteretic loops of the infilled wall frame structure under the generic harmonic signal acceleration, considering the stiffness and strength degradation with the pinching effect (Case 3): a) Mass Ratio of 5%; b) Mass Ratio of 10%; c) Mass Ratio of 15%; d) Mass Ratio of 20%.

Thus, pinching can be considered in the aforementioned numerical model by the following modification on the lateral stiffness of the frame, given by the following expression

$$k_f = ak_0 + \frac{k_{hyst}k_{slip-lock}}{k_{hyst} + k_{slip-lock}} \tag{5}$$

in which

$$k_{slip-lock} = \left\{ \sqrt{\frac{2}{\pi}} \frac{R_{sp}(\mu_d - 1)^{\kappa}\left(x_{max}^{+} - x_{max}^{-}\right)}{\sigma(1-a)P_{fy}} \exp - \left[0.5\left(\frac{P_f - \lambda_c P_{fy}}{\sigma P_{fy}} \right)^2 \right] \right\}^{-1} \qquad 0 \le R_{sp},\ \sigma,\ \lambda_c \le 1 \tag{6}$$

From Table 1, parameters R_{sp}, σ, κ and λ_c present in Eq. (6), are related to the pinching effect. this will be more evident for higher values of R_{sp} and lower values of σ.

The graphs from Figure 7 display the hysteretic cycles considering stiffness and strength degradation with the pinching effect. Each graph presents the controlled and uncontrolled hysteretic responses varying the value of the mass ratio.

Figure 8 presents the controlled and uncontrolled hysteretic loops only for the values μ=0.15; and μ=0.20, when the infilled wall frame structure is subjected to the seismic acceleration, considering the stiffness and strength degradation with the pinching effect.

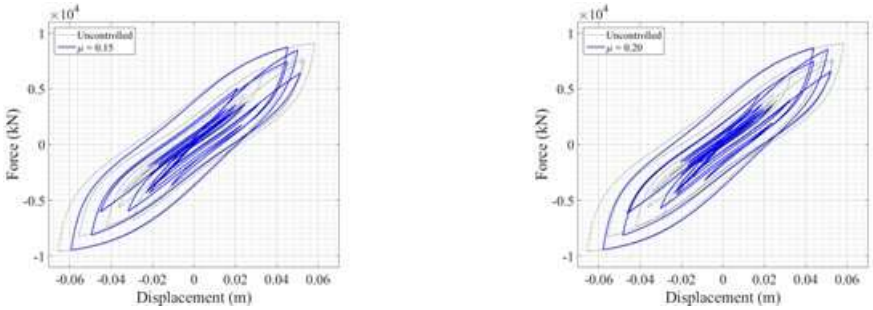

Fig. 8 – Hysteretic loops of the infilled wall frame structure under the seismic acceleration, considering the stiffness and strength degradation with the pinching effect (Case 3): a) Mass Ratio of 15%; b) Mass Ratio of 20%.

RESULTS

The results comprising the peak responses (displacement, velocity, acceleration and drift) are presented in form of tables. Considering the cases of hysteretic behaviour in study, Table 2 and Table 3 present the peak responses of the frame structure with or without infill wall and uncontrolled or controlled with the TMD, subjected to the generic harmonic signal and the seismic acceleration, respectively.

Table 2 shows that the presence of the infill wall in the uncontrolled frame structure offers great reductions of the peak responses and as one moves on to a more realistic case of hysteretic behaviour (from Case 0 to Case 3), smaller reductions of the peak responses relative to the uncontrolled frame structure without infill wall are being obtained.

Regarding the peak responses of the frame structure controlled with the TMD, it can be verified that the presence of the infill wall in the structure frame also offers significant reductions, and as in the previous paragraph smaller reductions are being obtained for more realistic cases of hysteretic behaviour, with the exception from Case 2 to 3 that presents a slightly bigger reduction. Thus, the TMD becomes less effective when Cases 2 and 3 of hysteretic behaviour are considered, rather than Cases 0 and 1.

As can be verified by the analysis of the hysteretic loops in Figures 4 to 8, the presence of the TMD will always reduce significantly the displacements of the structural system. The TMD also provides less contribution of the infilled wall frame structure in the energy dissipation (translated by the reduced area of the loops), avoiding a possible structural instability. The greater the mass ratio the less the displacements of the frame structure for almost the same values of its strength capacity. It can also be verified that the stiffness degradation becomes smaller for higher values of the mass ratio (translated by the slope of the loading and unloading curves).

Table 2 - Peak responses of the structure under the generic signal acceleration

Case of Hysteretic behaviour		*Mass ratio*	x (*m*)	$\dot{x}$ (*m/s*)	$\ddot{x}$ (*m/s²*)	drift (*m*)
Without infill wall		**0.00 (Uncontrolled)**	0.673	4.184	26.565	0.673
		0.05	0.301 (55%) 1.127	1.882 (55%) 6.719	11.795 (56%) 41.796	0.301 (55%) 1.064
		0.10	0.254 (62%) 0.681	1.584 (62%) 3.968	9.891 (63%) 24.758	0.254 (62%) 0.637
		0.15	0.233 (65%) 0.512	1.443 (66%) 2.947	9.007 (66%) 18.267	0.233 (65%) 0.484
		0.20	0.221 (67%) 0.431	1.363 (67%) 2.398	8.457 (68%) 14.821	0.221 (67%) 0.408
With infill wall	*Case 0*	**0.00 (Uncontrolled)**	0.145	0.860	6.357	0.145
		0.05	0.106 (27%) 0.567	0.643 (25%) 3.501	4.680 (26%) 21.910	0.106 (27%) 0.528
		0.10	0.101 (30%) 0.383	0.613 (29%) 2.383	4.453 (30%) 14.943	0.101 (30%) 0.355
		0.15	0.100 (31%) 0.311	0.604 (30%) 1.918	4.406 (31%) 11.997	0.100 (31%) 0.285
		0.20	0.100 (31%) 0.272	0.604 (30%) 1.659	4.393 (31%) 10.326	0.100 (31%) 0.247
	Case 1	**0.00 (Uncontrolled)**	0.186	1.134	7.722	0.186
		0.05	0.132 (29%) 0.661	0.819 (28%) 4.066	5.520 (29%) 25.237	0.132 (29%) 0.623
		0.10	0.123 (34%) 0.444	0.762 (33%) 2.730	5.158 (33%) 17.109	0.123 (34%) 0.414
		0.15	0.120 (36%) 0.353	0.743 (35%) 2.171	5.031 (35%) 13.576	0.120 (36%) 0.331
		0.20	0.119 (36%) 0.306	0.735 (35%) 1.862	4.987 (35%) 11.616	0.119 (36%) 0.286
	Case 2	**0.00 (Uncontrolled)**	0.433	2.929	24.342	0.433
		0.05	0.278 (36%) 1.027	1.699 (42%) 5.977	10.653 (56%) 35.704	0.278 (36%) 0.948
		0.10	0.227 (48%) 0.648	1.395 (52%) 3.697	8.739 (64%) 22.541	0.227 (48%) 0.594
		0.15	0.203 (53%) 0.493	1.252 (57%) 2.725	7.908 (68%) 16.796	0.203 (53%) 0.451
		0.20	0.192 (56%) 0.415	1.178 (60%) 2.209	7.460 (69%) 13.630	0.192 (56%) 0.378
	Case 3	**0.00 (Uncontrolled)**	0.545	3.373	27.055	0.545
		0.05	0.276 (49%) 1.046	1.686 (50%) 6.141	10.558 (61%) 36.966	0.276 (49%) 0.966
		0.10	0.224 (59%) 0.654	1.387 (59%) 3.776	8.705 (68%) 23.215	0.224 (59%) 0.601
		0.15	0.201 (63%) 0.496	1.248 (63%) 2.797	7.885 (71%) 17.272	0.201 (63%) 0.455
		0.20	0.190 (65%) 0.417	1.176 (65%) 2.297	7.446 (72%) 14.115	0.190 (65%) 0.381

The first and second lines represent the peak responses for the first and second floors, respectively, the main structure and the TMD. The percentage on the right of the values stands for the percentage of reduction of the peak responses with respect to the corresponding uncontrolled hysteretic case response.

Considering now an infilled wall structure in which it is applied a TMD, looking at the percentages on Table 2, the control action on the infilled wall structure reveals great reductions on the peak responses, and that these reductions are higher for more realistic cases of hysteretic behaviour.

On the values of the mass ratio between the TMD and the structure, it is evident that the higher the mass of the TMD the greater will be the reductions in relation to the respective uncontrolled hysteretic case.

Table 3 - Peak responses of the structure under the seismic acceleration of El Centro's earthquake

Case of Hysteretic behaviour		*Mass ratio*	*x (m)*	*ẋ (m/s)*	*ẍ (m/s²)*	**drift (*m*)**
Without infill wall		**0.00 (Uncontrolled)**	0.128	0.906	7.025	0.128
		0.05	0.093 (28%) 0.259	0.607 (33%) 1.646	5.181 (26%) 9.740	0.093 (28%) 0.259
		0.10	0.086 (33%) 0.189	0.592 (35%) 1.123	5.007 (29%) 6.977	0.086 (33%) 0.184
		0.15	0.081 (36%) 0.160	0.577 (36%) 0.922	4.854 (31%) 5.899	0.081 (36%) 0.147
		0.20	0.077 (40%) 0.141	0.562 (38%) 0.779	4.798 (32%) 5.108	0.077 (40%) 0.132
With infill wall	*Case 0*	**0.00 (Uncontrolled)**	0.064	0.627	6.391	0.064
		0.05	0.062 (4%) 0.146	0.618 (1%) 0.895	6.264 (2%) 6.294	0.062 (4%) 0.154
		0.10	0.059 (7%) 0.118	0.613 (2%) 0.740	6.130 (4%) 5.617	0.059 (7%) 0.124
		0.15	0.058 (10%) 0.101	0.610 (3%) 0.643	6.007 (6%) 5.206	0.058 (10%) 0.106
		0.20	0.056 (12%) 0.090	0.608 (3%) 0.574	5.899 (8%) 4.888	0.056 (12%) 0.094
	Case 1	**0.00 (Uncontrolled)**	0.066	0.636	6.381	0.066
		0.05	0.063 (4%) 0.155	0.628 (1%) 0.930	6.247 (2%) 6.695	0.063 (4%) 0.164
		0.10	0.061 (7%) 0.125	0.623 (2%) 0.771	6.105 (4%) 5.636	0.061 (7%) 0.132
		0.15	0.059 (10%) 0.108	0.620 (3%) 0.669	5.975 (6%) 5.218	0.059 (10%) 0.113
		0.20	0.058 (12%) 0.096	0.618 (3%) 0.597	5.868 (8%) 4.894	0.058 (12%) 0.101
	Case 2	**0.00 (Uncontrolled)**	0.066	0.635	6.353	0.066
		0.05	0.063 (4%) 0.156	0.627 (1%) 0.931	6.221 (2%) 6.705	0.063 (4%) 0.163
		0.10	0.061 (7%) 0.126	0.622 (2%) 0.771	6.081 (4%) 5.613	0.061 (7%) 0.132
		0.15	0.059 (10%) 0.109	0.619 (3%) 0.669	5.952 (6%) 5.196	0.059 (10%) 0.113
		0.20	0.058 (12%) 0.097	0.617 (3%) 0.596	5.837 (8%) 4.872	0.058 (12%) 0.100
	Case 3	**0.00 (Uncontrolled)**	0.066	0.635	6.353	0.066
		0.05	0.063 (4%) 0.162	0.627 (1%) 0.979	6.221 (2%) 6.979	0.063 (4%) 0.170
		0.10	0.061 (8%) 0.132	0.622 (2%) 0.788	6.081 (4%) 5.678	0.061 (8%) 0.138
		0.15	0.059 (10%) 0.114	0.619 (3%) 0.685	5.952 (6%) 5.200	0.059 (10%) 0.118
		0.20	0.058 (12%) 0.102	0.617 (3%) 0.612	5.837 (8%) 4.876	0.058 (12%) 0.105

The first and second lines represent the peak responses for the first and second floors, respectively, the main structure and the TMD. The percentage on the right of the values stands for the percentage of reduction of the peak responses with respect to the corresponding uncontrolled hysteretic case response.

Observing Table 3, considering now the seismic acceleration, the presence of the TMD also offers significant reductions and the same conclusions made for Table 2 for the generic harmonic signal can be withdrawn, although not as perceptive due to the high irregularity of the acceleration signal. There is a very slight reduction in the peak responses as one moves on to a more realistic case of hysteretic behaviour, so that the percentages of reduction remain the same.

In order to better address this analysis another evaluation criterion is suggested for further investigation. This new set of evaluation criteria comprising normalized and RMS (Root Mean Square) responses and also control requirements was used to complete the performance assessment of each controlled case of hysteretic behaviour.

The first three criteria (J_1, J_2, J_3) are based on peak responses. The next four criteria (J_4, J_5, J_6, J_7) are related with the RMS structural responses (see Table 4). In these equations, $|\cdot|$ denotes the absolute value and $\|\cdot\|$ is the L2 norm given by (Braz-César, 2015 [10])

$$||\cdot||=\sqrt{\frac{1}{t_f}\int_0^{t_f}[\cdot]^2\,dt} \tag{7}$$

where $t_f = t_{max}$ represent the total excitation duration and t_f represent a sufficient large time to allow the response to attenuate.

Table 4 - Evaluation criteria for the structural responses in terms of peak responses and RMS ratios

Evaluation criterion	***Description***
$J_1 = \max_{t,i}\left(\frac{\lvert x_{i,c}(t)\rvert}{\lvert x_{\max,u}(t)\rvert}\right)$	Maximum peak floor displacement ratio whereby the floor displacements over time are normalized by the maximum peak uncontrolled displacement.
$J_2 = \max_{t,i}\left(\frac{\lvert \dot{x}_{i,c}(t)\rvert}{\lvert \dot{x}_{\max,u}(t)\rvert}\right)$	Maximum peak floor velocity ratio whereby the floor velocities over time are normalized by the maximum peak uncontrolled velocity.
$J_3 = \max_{t,i}\left(\frac{\lvert \ddot{x}_{i,c}(t)\rvert}{\lvert \ddot{x}_{\max,u}(t)\rvert}\right)$	Maximum peak floor acceleration ratio whereby the floor accelerations over time are normalized by the maximum peak uncontrolled acceleration.
$J_4 = \max_{t,i}\left(\frac{\lVert x_{i,c}(t)\rVert}{\lVert x_{\max,u}(t)\rVert}\right)$	Maximum RMS floor displacement ratio, which is given in terms of the maximum RMS absolute displacement over time with respect to the uncontrolled case.
$J_5 = \max_{t,i}\left(\frac{\lVert \dot{x}_{i,c}(t)\rVert}{\lVert \dot{x}_{\max,u}(t)\rVert}\right)$	Maximum RMS floor velocity ratio, which is given in terms of the maximum RMS absolute velocity over time with respect to the uncontrolled case.
$J_6 = \max_{t,i}\left(\frac{\lVert \ddot{x}_{i,c}(t)\rVert}{\lVert \ddot{x}_{\max,u}(t)\rVert}\right)$	Maximum RMS floor acceleration ratio, which is given in terms of the maximum RMS absolute acceleration over time with respect to the uncontrolled case.
$J_7 = \max_{t,i}\left(\frac{\lVert d_{i,c}(t)\rVert}{\lVert d_{\max,u}(t)\rVert}\right)$	Maximum RMS inter-story drift ratio, which is given in terms of the maximum RMS absolute inter-story drift over time with respect to the uncontrolled case. Inter-story drift $d_i = \delta_i/h_i$.

Subscript $i = 1, 2$ denotes the story index and subscripts c and u represent controlled and uncontrolled cases.

One can say by the analysis of the data in Tables 5 and 6 that the presence of the non-structural element with hysteretic behaviour in the frame structure will influence its controlled response.

Observing Table 5, presenting the normalized peak and RMS responses for the generic harmonic signal acceleration, one can immediately conclude by the analysis of the percentage's values that smaller response reductions, whether it is peak or RMS responses, are obtained for the infilled wall frame structure with hysteretic behaviour concerning the stiffness and strength degradation with the pinching effect. This means that the more realistic is the hysteretic behaviour the lesser is the response reduction regarding the case without hysteretic behaviour or without the presence of the non-structural element.

Table 5 - Evaluation criteria values for the structural responses under the generic signal acceleration in terms of peak responses and RMS ratios

Evaluation criterion									
Case of Hysteretic behavior		***Mass ratio***	***Peak responses***			***RMS responses***			
			J_1	J_2	J_3	J_4	J_5	J_6	J_7
Without infill wall		**0.05**	1.673	0.450	1.573	1.600	1.575	1.555	1.542
		0.10	1.011	0.379	0.932	0.958	0.936	0.919	0.936
		0.15	0.761	0.345	0.688	0.714	0.693	0.679	0.714
		0.20	0.640	0.326	0.558	0.585	0.563	0.550	0.600
With infill wall	***Case 0***	**0.05**	0.842 (50%)	0.154 (66%)	0.825 (48%)	0.792 (50%)	0.781 (50%)	0.772 (50%)	0.748 (52%)
		0.10	0.570 (44%)	0.147 (61%)	0.563 (40%)	0.559 (42%)	0.549 (41%)	0.542 (41%)	0.523 (44%)
		0.15	0.462 (39%)	0.144 (58%)	0.452 (34%)	0.458 (36%)	0.448 (35%)	0.442 (35%)	0.427 (40%)
		0.20	0.404 (37%)	0.144 (56%)	0.389 (30%)	0.400 (32%)	0.389 (31%)	0.383 (30%)	0.372 (38%)
	Case 1	**0.05**	0.982 (41%)	0.196 (56%)	0.950 (40%)	0.856 (47%)	0.843 (46%)	0.833 (46%)	0.812 (47%)
		0.10	0.659 (35%)	0.182 (52%)	0.644 (31%)	0.602 (37%)	0.590 (37%)	0.582 (37%)	0.567 (39%)
		0.15	0.525 (31%)	0.178 (49%)	0.511 (26%)	0.492 (31%)	0.480 (31%)	0.473 (30%)	0.463 (35%)
		0.20	0.455 (29%)	0.176 (46%)	0.437 (22%)	0.429 (27%)	0.417 (26%)	0.410 (25%)	0.406 (32%)
	Case 2	**0.05**	1.525 (9%)	0.406 (10%)	1.344 (15%)	1.171 (27%)	1.128 (28%)	1.091 (30%)	1.082 (30%)
		0.10	0.962 (5%)	0.333 (12%)	0.849 (9%)	0.762 (20%)	0.729 (22%)	0.702 (24%)	0.704 (25%)
		0.15	0.732 (4%)	0.299 (13%)	0.632 (8%)	0.596 (16%)	0.568 (18%)	0.547 (19%)	0.556 (22%)
		0.20	0.616 (4%)	0.282 (14%)	0.513 (8%)	0.505 (14%)	0.479 (15%)	0.461 (16%)	0.478 (20%)
	Case 3	**0.05**	1.553 (7%)	0.403 (10%)	1.392 (12%)	1.214 (24%)	1.170 (26%)	1.133 (27%)	1.124 (27%)
		0.10	0.972 (4%)	0.331 (12%)	0.874 (6%)	0.790 (17%)	0.757 (19%)	0.731 (20%)	0.734 (22%)
		0.15	0.737 (3%)	0.298 (14%)	0.65 (5%)	0.618 (13%)	0.59 (15%)	0.569 (16%)	0.581 (19%)
		0.20	0.619 (3%)	0.281 (14%)	0.531 (5%)	0.523 (11%)	0.498 (12%)	0.480 (13%)	0.500 (17%)

The percentage below the values stands for the percentage of reduction of the peak responses with respect to the corresponding response without infill wall.

Although the TMD presents higher reductions of the structural responses for higher values of the mass ratio within the same case of hysteretic behaviour, the same does not happen when the several cases are compared with the case without infill wall. In this case, the TMD loses effectiveness when its mass is increased, i.e., when the mass ratio μ is increased, and as one moves one from Case 0 to Case 3. For instance, a structure with no infill walls controlled by a

TMD with 5% of the structure mass, will have a reduction of the maximum RMS floor displacement ratio of 7% when an infill wall with hysteretic behaviour of Case 3 is considered, on the other hand a structure with no infill walls controlled by a TMD with 20% of the structure mass, will only have a reduction of the maximum RMS floor displacement ratio of 3% when an infill wall with the same hysteretic behaviour is considered.

In Table 6, when the seismic acceleration signal is considered, the same conclusions made for Table 5 can be withdrawn, although sometimes not as perceptive.

Table 6 - Evaluation criteria values for the structural responses under the El Centro's signal acceleration in terms of peak responses and RMS ratios

Evaluation criterion									
Case of Hysteretic behavior		***Mass ratio***	***Peak responses***			***RMS responses***			
			J_1	J_2	J_3	J_4	J_5	J_6	J_7
Without infill wall		**0.05**	2.024	0.669	1.387	2.474	2.190	1.842	2.245
		0.10	1.473	0.653	0.993	1.833	1.549	1.281	1.614
		0.15	1.250	0.637	0.840	1.529	1.240	1.019	1.331
		0.20	1.103	0.620	0.727	1.377	1.069	0.871	1.185
With infill wall	***Case 0***	**0.05**	1.137 (44%)	0.682 (-2%)	0.896 (35%)	1.177 (52%)	1.191 (46%)	1.215 (34%)	1.321 (41%)
		0.10	0.918 (38%)	0.676 (-3%)	0.873 (12%)	0.970 (47%)	0.965 (38%)	1.001 (22%)	1.090 (33%)
		0.15	0.790 (37%)	0.673 (-6%)	0.855 (-2%)	0.867 (43%)	0.844 (32%)	0.902 (12%)	0.968 (27%)
		0.20	0.706 (36%)	0.671 (-8%)	0.840 (-15%)	0.806 (41%)	0.767 (28%)	0.880 (-1%)	0.892 (25%)
	Case 1	**0.05**	1.209 (40%)	0.693 (-3%)	0.953 (31%)	1.236 (50%)	1.240 (43%)	1.242 (33%)	1.379 (39%)
		0.10	0.980 (33%)	0.687 (-5%)	0.869 (12%)	1.015 (45%)	0.997 (36%)	1.012 (21%)	1.131 (30%)
		0.15	0.843 (33%)	0.684 (-7%)	0.851 (-1%)	0.906 (41%)	0.869 (30%)	0.897 (12%)	1.002 (25%)
		0.20	0.753 (32%)	0.682 (-10%)	0.835 (-15%)	0.842 (39%)	0.788 (26%)	0.876 (-1%)	0.922 (22%)
	Case 2	**0.05**	1.219 (40%)	0.692 (-3%)	0.955 (31%)	1.239 (50%)	1.236 (44%)	1.231 (33%)	1.362 (39%)
		0.10	0.988 (33%)	0.686 (-5%)	0.866 (13%)	1.017 (45%)	0.992 (36%)	1.001 (22%)	1.115 (31%)
		0.15	0.850 (32%)	0.683 (-7%)	0.847 (-1%)	0.907 (41%)	0.864 (30%)	0.878 (14%)	0.987 (26%)
		0.20	0.758 (31%)	0.681 (-10%)	0.831 (-14%)	0.843 (39%)	0.783 (27%)	0.857 (2%)	0.909 (23%)
	Case 3	**0.05**	1.266 (37%)	0.692 (-3%)	0.994 (28%)	1.336 (46%)	1.330 (39%)	1.305 (29%)	1.463 (35%)
		0.10	1.032 (30%)	0.686 (-5%)	0.866 (13%)	1.078 (41%)	1.044 (33%)	1.034 (19%)	1.169 (28%)
		0.15	0.891 (29%)	0.682 (-7%)	0.847 (-1%)	0.957 (37%)	0.902 (27%)	0.897 (12%)	1.027 (23%)
		0.20	0.799 (28%)	0.680 (-10%)	0.831 (-14%)	0.887 (36%)	0.815 (24%)	0.830 (5%)	0.943 (20%)

The percentage below the values stands for the percentage of reduction of the peak responses with respect to the corresponding response without infill wall.

It can be noted that due to the high irregularities of the seismic acceleration signal, the presence of the wall aggravates the structural response in some ways, observing increases in the maximum peak floor velocity and acceleration ratio, that are higher for bigger masses of the TMD.

The presence of the infill wall in the controlled structure also worsens the maximum RMS floor acceleration ratio for some situations where the TMD has 20% of the structure mass.

The best result for the mass ratio is 20%, presenting bigger peak responses reductions, when the system is subjected to the generic harmonic signal acceleration (Table 2). Observing the values of Table 3, the mass ratio that presents greater reductions is also 20%.

The hysteretic loops in Figures 4 to 8 also show the obvious effectiveness of the TMD in its control action and energy dissipation for the various hysteretic behaviour cases.

However, when analysing Tables 5 and 6, it was found that the presence of the infill wall in some particular responses could negatively influence the effectiveness of the TMD control action, especially for higher values of the mass ratio between the TMD and the structure.

Although the value of the mass ratio of 20% presents greater reductions, this may not be the best choice of the TMD design. This is because the mass ratio of 15% offers in some cases results that are in the least equal. Additionally, one must realize that applying more 5% of the structure mass will eventually need more structural reinforcement, which may not compensate the additional reduction of the peak responses that the 20% mass ratio has to offer in relation to the one of 15%. This can also be verified in the hysteretic loops that remain almost the same for 15% and 20% of the mass ratio.

CONCLUSIONS

The effectiveness of the TMD is evident when observing the reductions of the peak responses and the effect that has on the hysteretic loops in reducing the displacements for the same strength capacity of the infilled wall frame structure, preventing eventual structural instabilities.

The presence of non-structural elements shows very different results from the ones in which they are neglected. They offer more ductility and energy dissipation capability, but can bring serious problems if an out of the plane failure happens. It was verified that the implementation of the TMD can avoid this type of failure, reducing the ductility and energy dissipation demands on the infilled wall frame structure.

Although the mass ratio that provides the best results in peak reductions is the one of 20%, the mass ratio with 15% has almost the same results, less 5% of mass transmitted to the structure and in some particular cases offers better results, being this the optimal choice between the mass ratios considered in this study.

ACKNOWLEDGMENTS

The authors gratefully acknowledge the funding by Fundação para a Ciência e a Tecnologia (FCT), Portugal, through the funding of the phD studentship with reference SFRH/BD/ 139570/2018.

REFERENCES

[1] Folhento Pedro LP (2017), Dissertação de Mestrado. Estudo da Influência das Paredes de Alvenaria no Desempenho de Amortecedores de Massa Sintonizada. Instituto Politécnico de Bragança.

[2] Mousavi SA, Zahrai MS, Saatcioglu M (2015), Article. Toward Buckling Free Tension-Only Braces Using Slack Free Connections. Journal of Constructional Steel Research, Vol. 115, pp.329-345 - ELSEVIER.

[3] Bouc R (1967), Article. Forced Vibration of Mechanical Systems with Hysteresis. Proceedings 4th Conf. on Non-linear Oscillations.

[4] Wen Y-K (1976), Article. Method for Random Vibration of Vibration of Hysteretic Systems. J. Engrg. Mech. Div., ASCE, 102(2), pp.249-263.

[5] Baber TT, Noori MN (1985) Article. Random Vibration of Degrading, Pinching Systems. J. Engrg. Mech., ASCE, 111(8), pp.1010–1026.

[6] Casciati, F (1989), Article. Stochastic Dynamics of Hysteretic Media. Amsterdam: Struct. Safety, 6, pp.259-269.

[7] Reinhorn AM, Madan A, Valles RE, Reinchmann Y, Mander JB (1995), Technical Report NCEER-95-0018. Modeling of Masonry Infill Panels for Structural Analysis. State University of New York at Buffalo, Buffalo, N.Y.

[8] Sivaselvan MV, Reinhorn AM (2000), Article. Hysteretic Models for Deteriorating Ineslatic Structures. Journal of Engineering Mechanics, Vol. 126, Issue 6, pp.633-640.

[9] Park YJ, Ang AH-S, Wen YK (1987), Article. Damage – Limiting Aseismic Design of Buildings. Earthquake Spectra, Vol. 3, Nº1.

[10] Braz-César MT (2015), PhD Thesis in Civil/Structures Engineering. Vibration Control of Building Structures using MagnetoRheological Dampers. Porto, Portugal: Faculdade de Engenharia da Universidade do Porto.

[11] Braz-César M, Oliveira D, Barros R (2013), Validação Numérica da Resposta Cíclica Experimental de Pórticos de Betão Armado (in portuguese). Revista da Associação Portuguesa de Análise Experimental de Tensões - Mecânica Experimental, 22, pp.1-13.

.